

## ARTICLE

# Nonlinear Optical Properties of D- $\pi$ -A- $\pi$ -D Type Oligomers with Different Conjugation Length

Tian-hao Huang<sup>a,b</sup>, Ying-hui Wang<sup>b</sup>, Tian-ning Xu<sup>a\*</sup>, Feng-ying Yu<sup>a</sup>, Han-zhuang Zhang<sup>b</sup>, Yu-ran Wang<sup>c</sup>

*a.* Department of Science, Zhijiang College of Zhejiang University of Technology, Hangzhou 310024, China

*b.* Femtosecond Laboratory, College of Physics, Jilin University, Changchun 130012, China

*c.* North China University of Science and Technology, Tangshan 063000, China

(Dated: Received on April 11, 2015; Accepted on May 13, 2015)

The conjugation length-dependent nonlinear optical properties of fluorenone-based linear conjugated oligomers have been investigated by experimental and theoretical methods. Infrared spectra and the steady-state absorption spectra show that the increase of conjugated unit could enhance the stretching vibration peaks of C=C and lead to a red-shift of the absorption peaks. Meanwhile, the two-photon fluorescence (TPF) intensity is gradually enhanced with the increase of excitation energy, and the TPF efficiency is obviously higher after the introduction of fluorene-ethylene units. The sum-over-states approach was used to model the two-photon absorption (TPA) cross-sections of oligomers, and the theoretical values agree well with the experimental data obtained from the femtosecond open-aperture *z*-scan technique. The results exhibit that the extension of conjugated system indeed plays a role in the improvement of TPA behavior of oligomers.

**Key words:** Linear conjugated oligomer, Two-photo absorption, Sum-over-states

## I. INTRODUCTION

$\pi$ -conjugated organic oligomers with donor-acceptor (D-A) architectures have attracted much attention [1–5], because they can be used as the active elements for organic electronic and optoelectronic devices, such as organic light-emitting diodes (OLEDs) [6, 7], solar cells [8, 9], field-effect transistors (FETs) [10, 11], organic photovoltaic devices (OPVs) [12, 13] and electrical conductors [14, 15]. The monodispersed, well defined  $\pi$ -conjugated oligomers acting as model molecules are beneficial to understand the fundamental properties of the related polymers as well as the structure-property relationship [16, 17]. D-A  $\pi$ -conjugated oligomers involve two types: asymmetrical D- $\pi$ -A type and symmetrical D- $\pi$ -A- $\pi$ -D or A- $\pi$ -D- $\pi$ -A type, and their properties can be easily modified through modulating donor or acceptor moieties. As we know, in spite of many reports on the asymmetrical D-A structures, investigations on the symmetrical D-A structures are relatively less [18–20]. The major reason is that the synthesis of symmetrical D-A molecules is more complicated than that of the asymmetrical ones, and thus the separation and purification become more difficult. However, as compared

with the asymmetrical D-A molecules, the symmetrical ones can lead to a more effective intramolecular charge transfer (ICT), which is favorable to long wave emission and an excellent nonlinear optical property.

Two-photon absorption (TPA) is a nonlinear optical process in which the molecules were excited to a higher-energy state by absorbing two photons simultaneously, with the energy being equal to the sum of the energies of the two photons absorbed. Much efforts have been devoted to the conjugated oligomers with excellent TPA property because of their potential utility in two-photon fluorescence microscopy [21], two-photon photodynamic therapy [22], optical limiting [23, 24], 3D micro-fabrication and optical data storage [25–28]. Many methods have been used to investigate the TPA property of molecules, such as two-photon induced fluorescence [29], open-aperture *z*-scan technique [30], nonlinear transmission method [31], and two-photon transient absorption spectroscopy [32]. It has been reported that increasing the donor-acceptor strength, introducing coplanar  $\pi$ -spacer group or extending the conjugation length of oligomers are effective ways for designing conjugated oligomers with enhanced TPA behavior.

In this work, nonlinear optical properties of two D- $\pi$ -A- $\pi$ -D type linear conjugated oligomers 2,7-di(*E*)-2-(9,9-dioctyl-9H-fluoren-2-yl)vinyl)-9-fluorenone (F-F O-F) and 2,7-di(*E*)-2-(7-(*E*)-2-(9,9-dioctyl-9H-fluoren-2-yl)vinyl)-9,9-dioctyl-9H-fluoren-2-yl)vinyl)-9-fluorenone (F-F-FO-F-F), where fluorenone and fluorene

\* Author to whom correspondence should be addressed. E-mail: xutianning@zjut.edu.cn

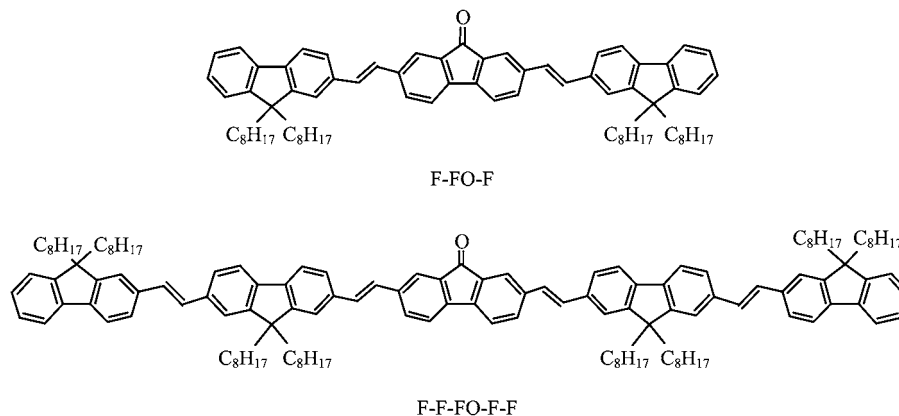


FIG. 1 Molecular structures of F-FO-F and F-F-FO-F-F.

act as the electron acceptor and donor respectively have been investigated. In comparison with F-FO-F, fluorene-ethylene (FE) as  $\pi$ -spacer groups were introduced between the acceptor and donor moieties for F-F-FO-F-F, which can simultaneously lead to the enhancement of molecular coplanarity and the extension of conjugated system. Two-photon fluorescence (TPF) and femtosecond open-aperture  $z$ -scan technique were employed to experimentally study the conjugated length-dependent two-photon optical properties of the oligomers. Meanwhile, the theoretical results of TPA cross-section were simulated by employing the sum-over-states (SOS) approach, and a five-energy-level diagram was plotted to describe the TPA process. This study can provide a deep insight into the structure-property relationship of the conjugated oligomers with two-photon optical properties.

## II. EXPERIMENTS

The oligomers F-FO-F and F-F-FO-F-F, as shown in Fig.1, were both synthesized via Heck reaction, and the synthetic procedures have been reported previously [33, 34]. Toluene solutions of both oligomers were prepared with concentrations of  $5 \times 10^{-5}$  mol/L in 5 mm thick quartz cuvette and  $5.0 \times 10^{-4}$  mol/L in 2 mm thick quartz cuvette, for linear and nonlinear optical measurements, respectively. The infrared (IR) spectra were measured by a Germany Bruker Vertex 80v FT-IR spectrometer. Steady-state absorption spectra were measured with an AvaSpec-2048 bi-pass fiber spectrometer (Avantes). Nonlinear optical measurements were performed using a mode-lock Ti:sapphire femtosecond laser (Coherent). The amplified pulses of 2.2 mJ, 130 fs at 800 nm with a repetition rate of 1 kHz can be obtained. TPF spectra were obtained using a fiber optic spectrometer (Ocean Optics 4000). The TPA cross-sections were experimentally measured by the femtosecond open-aperture  $z$ -scan technique, the details of

TABLE I Characteristic vibrational frequencies of F-FO-F and F-F-FO-F-F.

Assignment/cm <sup>-1</sup>	F-FO-F	F-F-FO-F-F
$\nu_{as}(\text{CH}_2)$	2926	2925
$\nu_s(\text{CH}_2)$	2853	2853
$\nu(\text{C}=\text{O})$	1713	1711
$\nu(\text{C}=\text{C})$	1637	1635
$\delta_{as}(\text{CH}_3)$	1465	1464
$\delta_s(\text{CH}_3)$	1385	1385
$\delta(=\text{C}-\text{H})$	962	963
$\delta(=\text{C}-\text{H})$	740	738

which have been reported before [33].

## III. RESULTS AND DISCUSSION

To confirm the molecular structures of the oligomers, the IR spectra were measured. As shown in Fig.2, IR spectra exhibit the characteristic vibrational peaks of oligomers. The characteristic frequencies and their assignments are listed in Table I. The oligomers show obvious  $\text{CH}_2$  asymmetrical stretching  $\nu_{as}(\text{CH}_2)$  and symmetrical stretching  $\nu_s(\text{CH}_2)$  peaks due to their massive methylene groups. Besides, the stretching vibration peak of  $\text{C}=\text{C}$   $\nu(\text{C}=\text{C})$  is significantly enhanced in F-F-FO-F-F with  $\text{C}=\text{C}$  prolonging. It is noteworthy that the oligomers exhibit IR absorption bands near  $960 \text{ cm}^{-1}$  belonging to the wagging vibration [35] of the *trans*-double bond ( $\text{C}=\text{C}$ ). The *trans*-form compounds have good planarity, which is beneficial to the improvement of the fluorescence property.

Figure 3 shows the steady-state absorption spectra of oligomers, which were fitted by multi-peaks Gaussian. For both oligomers, the absorption spectra are mainly characterized by two bands. One near 300–420 nm is assigned to the  $\pi$ - $\pi^*$  transition, and the other at around

TABLE II Spectroscopic parameters ( $\nu$  in  $\text{cm}^{-1}$ (nm),  $\Gamma$  in  $\text{cm}^{-1}$ ,  $\mu$  in Debye,  $\sigma$  in  $10^3\text{GM}$ ) used in the sum-over-states approach, employing the five-energy-level diagram.

$\nu$	F-FO-F	F-F-FO-F-F	$\Gamma$	F-FO-F	F-F-FO-F-F	$\mu$	F-FO-F	F-F-FO-F-F	$\sigma^a$	F-FO-F	F-F-FO-F-F
$\nu_{10}$	21186 (472.0)	20855 (479.5)	$\Gamma_{10}$	2941	3344	$\mu_{10}$	6.4	9.3	$\sigma_T^{(2)}$	0.74	1.81
$\nu_{20}$	24691 (404.6)	23348 (428.3)	$\Gamma_{20}$	6916	8130	$\mu_{21}$	5.5	8.8	$\sigma_E^{(2)}$	0.63	1.56
$\nu_{30}$	26110 (382.6)	24582 (406.8)	$\Gamma_{30}$	3077	3584	$\mu_{31}$	8.3	8.1			
$\nu_{40}$	31447 (318.3)	27412 (364.8)	$\Gamma_{40}$	3165	1456	$\mu_{41}$	2.5	1.1			

<sup>a</sup>  $\sigma_T^{(2)}$  and  $\sigma_E^{(2)}$  are the theoretical and experimental TPA cross-section values, respectively.

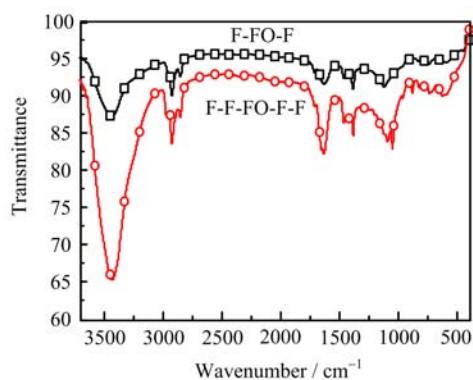


FIG. 2 IR spectra of F-FO-F and F-F-FO-F-F.

490 nm is largely of charge transfer transition. It is observed that the absorption spectra of F-F-FO-F-F presents significant red-shift with respect to F-FO-F due to the increase of the conjugation length, and the optical density is obviously increased as well. After several attempts, we found that the 4-peaks model fitted the experimental data quite well. The fitted results are summarized in Table II, which will be used in the theoretical calculation of the TPA cross-section, and the fitting details will be described later. The fitting results show that the first Gaussian peak of F-FO-F and F-F-FO-F-F are located at 472.0 and 479.5 nm, respectively, correspond with the charge transfer transition band, and the other three Gaussian peaks of F-FO-F (404.6, 382.6, 318.3 nm) and F-F-FO-F-F (428.3, 406.8, 364.8 nm) correspond with the  $\pi$ - $\pi^*$  transition band. Each Gaussian peak value of F-F-FO-F-F is red-shifted in comparison with that of F-FO-F.

The excitation intensity-dependent photoluminescence (PL) spectra of F-FO-F and F-F-FO-F-F are shown in Fig.4 (a) and (b), respectively. The wavelength of excitation laser is 800 nm, with the excitation energy increasing from 35  $\mu\text{J}$  to 80  $\mu\text{J}$ . It is observed that the fluorescence intensities of both oligomers are gradually enhanced with the increase of excitation energy. Meanwhile, as the conjugation length prolongs, the PL spectra of F-F-FO-F-F are slightly red-shifted relative to that of F-FO-F. Figure 4(c) shows that the integrated PL intensity of F-FO-F and F-F-FO-F-F

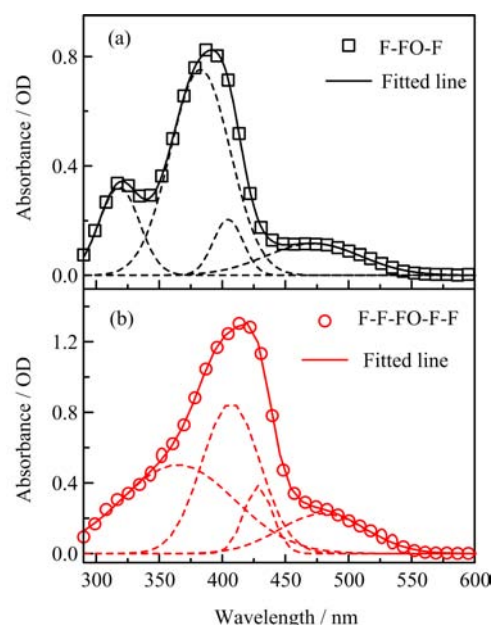


FIG. 3 Steady-state absorption spectra of F-FO-F and F-F-FO-F-F. The solid lines represent the fitted Gaussian line-shape and offer the spectroscopic parameters to use in the sum-over-states approach.

are linearly dependent on the square of the excitation-intensity, which confirms the TPA process at 800 nm. We can also see that the slope for F-F-FO-F-F is much larger than that for F-FO-F, demonstrating a much faster growth rate of PL intensity with the increasing of excitation energy. This phenomenon is indicative of an improved PL performance caused by the increase of the conjugation length. According to the equation  $I_{\text{TPF}} = S\delta\psi I_{800}^2$  here  $S$  is the intensity of the signal collected by the spectrometer,  $\delta$  is the overall fluorescence collection efficiency of the experimental apparatus,  $\psi$  is the TPF efficiency of samples [36], we can calculate that the TPF efficiency of F-F-FO-F-F is 3.7 times higher than that of F-FO-F, manifesting that a better nonlinear optical property could be achieved by the extension of conjugated system.

In order to further understand the relationship between the molecular structure and the TPA properties,

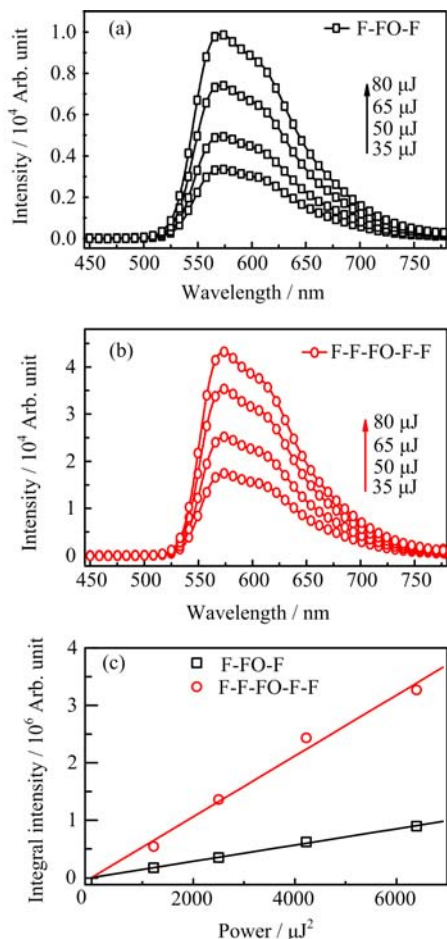


FIG. 4 Excitation energy dependent PL spectra of (a) F-FO-F and (b) F-F-FO-F-F excited by 800 nm femtosecond pulse, with the energy increasing of 35, 50, 65, 80  $\mu\text{J}$ , (c) the PL integral intensities of F-FO-F and F-F-FO-F-F as a function of the square of the laser energy.

we use SOS model to calculate the TPA cross-section of oligomers. As described above, most of the spectral parameters used in this model can be obtained from the Gaussian fitting of the steady-state absorption spectra, including the transition frequency ( $\nu$ ) and the damping factor ( $\Gamma$ ). We assume that the absorption bands of the oligomers exhibit Gaussian line-shape given by the following [37]:

$$g_{m0}(\omega) = 2\sqrt{\frac{\ln 2}{\pi}} \frac{A_{m0}}{\Gamma_{m0}} \exp\left[-4 \ln 2 \left(\frac{\omega_{m0} - \omega}{\Gamma_{m0}}\right)^2\right] \quad (1)$$

where  $A_{m0}$ ,  $\Gamma_{m0}$  and  $\omega_{m0}$  are the amplitude, the full width at half-maximum and the center frequency of the Gaussian line-shape, respectively. Meanwhile,  $\Gamma_{m0}$  represents the damping constant of the  $m$  state,  $\omega_{m0}$  represents the transition frequency between the  $m$  state and the ground state. The obtained spectroscopic parameters are summarized in Table II,  $\nu_{m0} = \omega_{m0}/2\pi$ .

To reduce the number of adjustable parameters, the transition dipole moments of oligomers could be determined using the steady-state absorption spectra. The transition moment vector of the  $m$  state ( $|\mu_{m0}\rangle$ ) can be calculated as follows:

$$|\mu_{m0}| = \sqrt{\frac{3}{4\pi} \frac{c}{\pi^{1/2}} \sigma_{m0}^{\max} \frac{\Gamma_{m0}}{2(\ln 2)^{1/2}} \frac{h}{\nu_{m0}}} \quad (2)$$

where  $c$  is the speed of light,  $h$  is the Planck's constant,  $\sigma_{m0}^{\max}$  is the maximum one-photon absorption cross-section of the  $m$  state, which can be calculated from:

$$\sigma = \frac{\varepsilon}{N_A} \ln 10 \quad (3)$$

where  $N_A$  is the Avogadro's constant,  $\varepsilon$  is the molar absorption coefficient, which can be obtained from  $D = \varepsilon cl$ , here  $D$  is the optical density,  $c$  is the concentration of oligomer solution, and  $l$  is the length of optical-path.

According to the Gaussian fitting, we assume that both oligomers have five states, an initial state ( $S_0$ ), an intermediate state ( $S_1$ ) and three final states ( $S_2$ ,  $S_3$  and  $S_4$ ). Assuming that the dipole moments are parallel to each other, the TPA cross-section can be written as follows [38]:

$$\sigma^{(2)} = \frac{4}{5\pi} \frac{(2\pi)^4}{(ch)^2} \frac{\nu_p^2}{(\nu_{10} - \nu_p)^2 + \Gamma_{10}^2} \left[ \frac{|\mu_{21}|^2 |\mu_{10}|^2 \Gamma_{20}}{(\nu_{20} - 2\nu_p)^2 + \Gamma_{20}^2} + \frac{|\mu_{31}|^2 |\mu_{10}|^2 \Gamma_{30}}{(\nu_{30} - 2\nu_p)^2 + \Gamma_{30}^2} + \frac{|\mu_{41}|^2 |\mu_{10}|^2 \Gamma_{40}}{(\nu_{40} - 2\nu_p)^2 + \Gamma_{40}^2} \right] \quad (4)$$

where  $\nu_{m0}$  ( $m=1-4$ ) is the transition frequency of the  $S_0 \rightarrow S_m$  transition,  $\nu_p$  is the laser frequency,  $|\mu_{m1}| = |\mu_{m0} - \mu_{10}|$  ( $m=2-4$ ).

In this way, a theoretical approximation of TPA cross-section ( $\sigma_T^{(2)}$ ) can be obtained. The calculated  $\sigma_T^{(2)}$  values, together with the corresponding spectroscopic parameters used in the SOS approach, are shown in Table II. The  $\sigma_T^{(2)}$  values of F-FO-F and F-F-FO-F-F are  $0.74 \times 10^3$  and  $1.81 \times 10^3$  GM, respectively, and the latter is 2.45 times larger than the former. This result indicates that the increasing of conjugated unit is beneficial for the enhancement of TPA cross-section.

The diagram of five-energy-level, which describes the TPA process under the SOS approach, is shown in Fig.5. Meanwhile, the energy-level values expressed by the transition frequency ( $\nu_{m0}$ ) are listed in Table II, which have already been obtained from the Gaussian fitting. It is observed that the dipole moment between the ground state ( $S_0$ ) and the first excited state ( $S_1$ ) are higher for F-F-FO-F-F, which could lead to a better ICT character in this oligomer with larger conjugation length. Moreover, as the absorption spectra of F-F-FO-F-F shows a red-shift behavior relative to that

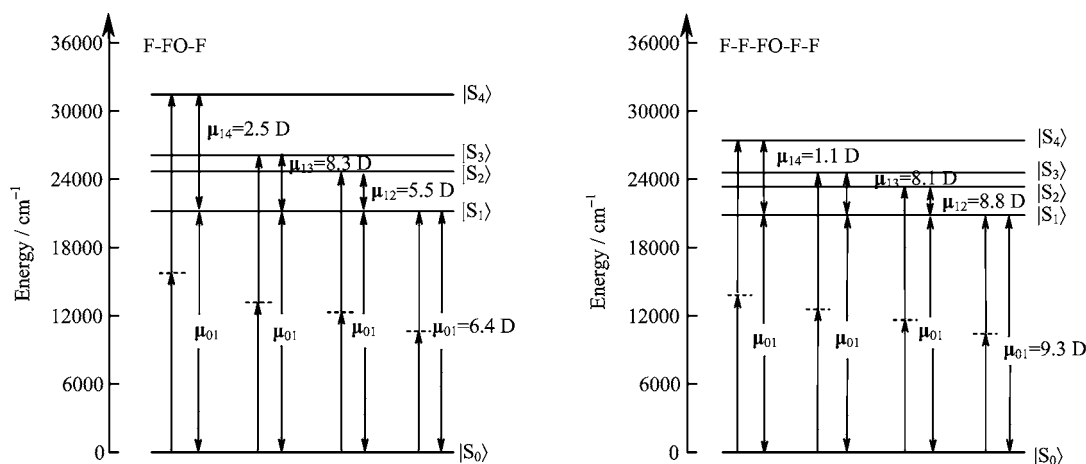


FIG. 5 Five-energy-level diagram for F-FO-F and F-F-FO-F-F used to describe the TPA process under the sum-over-states approach.

of F-FO-F, the decrease in band gap will contribute to the resonance enhancement of the TPA cross-section.

In order to support the results of the theoretical method, we offer the experimental results of the TPA cross-sections  $\sigma_E^{(2)}$ . The TPA cross-sections of F-FO-F and F-F-FO-F-F were measured by using femtosecond open-aperture  $z$ -scan technique, and the results are shown in Fig.6. The  $z$ -scan data of pure toluene solvent confirm that the influence of the solvent nonlinearity could be excluded. The experimental data can be fitted with the equation [39]:

$$T(z, S=1) = \sum_{m=0}^{\infty} \frac{[-q_0(z, 0)]^m}{(m+1)^{3/2}} \quad (5)$$

$$q_0(z) = \frac{\beta I_0}{1 + z^2/z_0^2} \quad (6)$$

where  $I_0$  is the pulse irradiance,  $z_0 = k\omega_0^2/2$  is the Rayleigh length ( $k=2\pi/\lambda$  is the wave vector,  $\omega_0$  is beam waist radius of Gaussian pulse). From Fig.6, the nonlinear coefficient  $\beta$  could be obtained. Finally, the TPA cross-sections  $\sigma_E^{(2)}$  can be calculated from  $\sigma^{(2)} = h\nu\beta/N$ , where  $N$  is the number of molecules per  $\text{cm}^3$ , and  $\sigma^{(2)}$  is expressed. The obtained  $\sigma_E^{(2)}$  values are  $0.63 \times 10^3$  and  $1.56 \times 10^3$  GM for F-FO-F and F-F-FO-F-F respectively, and the latter is almost 2.48 times higher than the former.

As described above, the experimental values  $\sigma_E^{(2)}$  are slightly smaller than the theoretical values  $\sigma_T^{(2)}$ , which may be caused by the acceptable detection error in the experiment. Besides, the theoretical and experimental values of TPA cross-section for F-F-FO-F-F are 2.45 and 2.48 times higher than those for F-FO-F, and the multiples are found to be similar to each other. Anyway, the results show that the  $\sigma_E^{(2)}$  values are intensely close to the  $\sigma_T^{(2)}$  values, and they exhibit similar enhancement

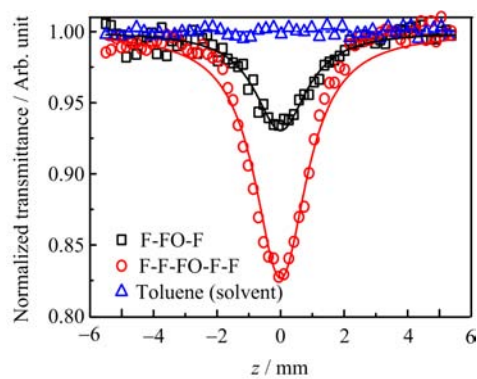


FIG. 6 Open-aperture  $z$ -scan curves for F-FO-F and F-F-FO-F-F in toluene. The solid lines represent the fitting results used to extract the nonlinear absorption coefficient.

behavior with the increasing of conjugated length.

#### IV. CONCLUSION

We have investigated the conjugated length-dependent nonlinear optical properties of two fluorenone-based D- $\pi$ -A- $\pi$ -D type linear conjugated oligomers. Firstly, the characteristic vibrational frequencies of oligomers were shown in IR spectra, which confirmed the molecular structures. The excitation intensity-dependent TPF spectra show that the introduction of FE units could increase the TPF efficiency. Moreover, the TPA cross-sections of oligomers were theoretically and experimentally studied by using SOS approach and femtosecond open-aperture  $z$ -scan technique, respectively. The results exhibit that the theoretical and experimental values are in good agreement with each other, and the extension of conjugated length could enhance the TPA cross-section

of the organic conjugated oligomers. In a word, this study could provide a useful guideline for the design of oligomers with enhanced TPA properties.

## V. ACKNOWLEDGMENTS

This work was supported by the National Natural Science Foundation of China (No.11274142) and the Doctoral Scientific Research Starting Foundation of Zhijiang College of Zhejiang University of Technology (No.108040120).

- [1] R. M. Metzger, *J. Mater. Chem.* **9**, 2027 (1999).
- [2] M. S. Wong, H. L. Zhong, Y. Tao, and M. D'Iorio, *Chem. Mater.* **15**, 1198 (2003).
- [3] J. Gierschner, J. Cornil, and H. J. Egelhaaf, *Adv. Mater.* **19**, 173 (2007).
- [4] A. Ajayaghosh, V. K. Praveen, S. Srinivasan, and R. Varghese, *Adv. Mater.* **19**, 411 (2007).
- [5] A. P. Kulkarni, Y. Zhu, and S. A. Jenekhe, *Macromolecules* **41**, 339 (2008).
- [6] P. F. Van Hutten, J. Wildeman, A. Meetsma, and G. Hadziioannou, *J. Am. Chem. Soc.* **121**, 5910 (1999).
- [7] U. Mitschke and P. Bauerle, *J. Mater. Chem.* **10**, 1471 (2000).
- [8] H. Hoppe and N. S. Sariciftci, *J. Mater. Res.* **19**, 1924 (2004).
- [9] J. L. Segura, N. Martn, and D. M. Guldi, *Chem. Soc. Rev.* **34**, 31 (2005).
- [10] F. Garnier, *Acc. Chem. Res.* **32**, 209 (1999).
- [11] G. Horowitz, *J. Mater. Chem.* **9**, 2021 (1999).
- [12] J. F. Nierengarten, *Sol. Energy Mater. Sol. Cells* **83**, 187 (2004).
- [13] F. Guo, K. Ogawa, Y. G. Kim, E. O. Danilov, F. N. Castellano, J. R. Reynolds, and K. S. Schanze, *Phys. Chem. Chem. Phys.* **9**, 2724 (2007).
- [14] H. Nakanishi, N. Sumi, Y. Aso, and T. Otsubo, *J. Org. Chem.* **63**, 8632 (1998).
- [15] H. Nakanishi, N. Sumi, S. Ueno, K. Takimiya, Y. Aso, T. Otsubo, K. Komaguchi, M. Shiotani, and N. Ohta, *Synth. Met.* **119**, 413 (2001).
- [16] S. S. Zade and M. Bendikov, *Org. Lett.* **8**, 5243 (2006).
- [17] K. Knoblack, C. Silvestri, and D. Collard, *J. Am. Chem. Soc.* **128**, 13680 (2006).
- [18] L. Xue, J. He, X. Gu, Z. Yang, B. Xu, and W. Tian, *J. Phys. Chem. C* **113**, 12911 (2009).
- [19] N. Pucher, A. Rosspeintner, V. Satzinger, V. Schmidt, G. Gescheidt, J. Stampfl, and R. Liska, *Macromolecules* **42**, 6519 (2009).
- [20] J. L. Wang, Q. Xiao, and J. Pei, *Org. Lett.* **12**, 18 (2010).
- [21] M. C. Skala, J. M. Squirrell, K. M. Vrotsos, V. C. Eickhoff, A. Gendron-Fitzpatrick, K. W. Eliceiri, and N. Ramanujam, *Cancer Res.* **65**, 1180 (2005).
- [22] D. Gao, R. R. Agayan, H. Xu, M. A. Philbert, and R. Kopelman, *Nano Lett.* **6**, 2383 (2006).
- [23] C. W. Spangler, *J. Mater. Chem.* **9**, 2013 (1999).
- [24] M. Calvete, G. Y. Yang, and M. Hanack, *Synth. Met.* **141**, 231 (2004).
- [25] D. A. Parthenopoulos and P. M. Rentzepis, *Science* **245**, 843 (1989).
- [26] S. Kawata and Y. Kawata, *Chem. Rev.* **100**, 1777 (2000).
- [27] S. Kawata, H. B. Sun, T. Tanaka, and K. Takada, *Nature* **412**, 697 (2001).
- [28] W. Zhou, S. M. Kuebler, K. L. Braun, T. Yu, J. K. Cammack, C. K. Ober, J. W. Perry, and S. R. Marder, *Science* **296**, 1106 (2002).
- [29] Z. P. Chen, D. L. Kaplan, K. Yang, J. Kumar, K. A. Marx, and S. K. Tripathy, *Appl. Opt.* **36**, 1655 (1997).
- [30] M. Sheik-Bahae, A. A. Said, and E. W. Van Stryland, *Opt. Lett.* **14**, 955 (1989).
- [31] T. F. Boggess, K. M. Bohnert, K. Mansour, S. C. Moss, I. W. Boyd, and A. L. Smirl, *IEEE J. Quant. Electron.* **22**, 360 (1986).
- [32] D. A. Oulianov, I. V. Tomov, A. S. Dvornikov, and P. M. Rentzepis, *Opt. Commun.* **191**, 235 (2001).
- [33] T. H. Huang, D. Yang, Z. H. Kang, E. L. Miao, R. Lu, H. P. Zhou, F. Wang, G. W. Wang, P. F. Cheng, Y. H. Wang, and H. Z. Zhang, *Opt. Mater.* **35**, 467 (2013).
- [34] T. H. Huang, X. C. Li, Y. H. Wang, Z. H. Kang, R. Lu, E. L. Miao, F. Wang, G. W. Wang, and H. Z. Zhang, *Opt. Mater.* **35**, 1373 (2013).
- [35] X. Qiu, R. Lu, H. Zhou, X. Zhang, T. Xu, X. Liu, and Y. Zhao, *Tetrahedron Lett.* **48**, 7582 (2007).
- [36] L. Gong, Y. Wang, Z. Kang, T. Huang, R. Lu, and H. Zhang, *Chin. J. Chem. Phys.* **25**, 643 (2012).
- [37] M. G. Vivas, S. L. Nogueira, H. Santos Silva, N. M. Barbosa Neto, A. Marletta, F. Serein-Spirau, S. Lois, T. Jarrosson, L. De Boni, R. A. Silva, and C. R. Mendonca, *J. Phys. Chem. B* **115**, 12687 (2011).
- [38] K. Kamada, K. Ohta, I. Yoichiro, and K. Kondo, *Chem. Phys. Lett.* **372**, 386 (2003).
- [39] M. Sheik-Bahae, A. A. Said, T. H. Wei, D. J. Hagan, and E. W. Van Stryland, *IEEE J. Quantum Electron.* **26**, 760 (1990).